J Mater Sci: Mater Electron (2016) 27:10993–11002
DOI 10.1007/s10854-016-5215-9

Investigation of the dielectric relaxation, conductivity and energy storage properties for biaxially oriented poly(vinylidene fluoride-hexafluoropropylene)/poly(methyl methacrylate) composite films by dielectric relaxation spectroscopy

Xiaojia Zhao[1] · Xubo Jiang[1] · Guirong Peng[1] · Wenpei Liu[1] · Ke Liu[1] · Zaiji Zhan[1]

Received: 26 May 2016 / Accepted: 17 June 2016 / Published online: 24 June 2016

Abstract The dielectric relaxations in biaxially oriented P(VDF-HFP)/PMMA composite films with less than 40 % PMMA were investigated using dielectric relaxation spectroscopy. Various relaxation processes and their locations of P(VDF-HFP), PMMA, and P(VDF-HFP)/PMMA composite films were analyzed. According to the fitted data of the Havriliak–Negami (HN) function, different relaxation processes belong to non-debye relaxation, the activation energy (E_a) and dielectric relaxation strength ($\Delta\varepsilon$) of P(VDF-HFP)/PMMA composite films significantly decreased around and above glass transition temperature (T_g) with increasing PMMA content. In addition, the conductivities (σ) of P(VDF-HFP)/PMMA composite films also sharply decreased with the addition of PMMA. The decrease of dielectric relaxation strength ($\Delta\varepsilon$) benefits the drop of P_r, lower the activation energy (E_a) makes coercive field decrease and the lower conductivity (σ) could enhances the breakdown strength. Thus, dielectric film of high energy storage density and low loss was closely related with the lower E_a, $\Delta\varepsilon$ and σ.

1 Introduction

Electroactive poly(vinylidene fluoride) (PVDF) and its copolymers show excellent mechanical properties, high thermal and chemical stability, strong piezoelectricity, pyroelectricity and ferroelectric responses, providing a wide range of applications [1, 2]. However, their typical dielectric loss is larger at ambient temperature because of dipole relaxation [3]. More importantly, they exhibit nonlinear dielectric and ferroelectric behaviors with nonlinear permittivity [4, 5], which results the decreases of energy storage density. For improving PVDF and its copolymers performance, several methods have been attempted, such as uniaxial tension [6, 7], grafting [8] and blending [9]. Among these methods, blending has the advantage of easily performing and realizing industrially.

PVDF and its copolymers are usually blended with oxygen-containing hydrophilic polymers such as poly (methyl methacrylate) (PMMA) to make blends with desired strength and electric properties [10, 11]. PVDF (or its copolymers)/PMMA blends are completely miscible in the melt state at all compositions, because of dipole–dipole interactions between PMMA and PVDF (or its copolymers) [12–14]. Thus, PVDF/PMMA blends have been widely studied. Zuo et al. [15] reported that the reduced cooperative domain sizes in the PVDF interphase and crystallites accelerated the VFT- and Arrhenius-type of α_a and α_c relaxations. Zhang [16] and Zhu et al. [17] investigated the presence of PMMA was in favor of the β phase transformation, but higher blending degree of PMMA could not increased the formation of β phase further. Peng [18] and Li [19] et al. reported that discharge efficiency of PVDF/PMMA blends markedly increased, and the polarization of PVDF/PMMA blends was much more stable than that of PVDF. To date, the study of the relationship between dielectric relaxation and electric energy density has not been reported.

Usually the preparation methods of PVDF/PMMA blends in these reports are solution casting and uniaxial tension. Biaxially oriented PVDF/PMMA composite films

✉ Guirong Peng
gr8599@aliyun.com

✉ Zaiji Zhan
zjzhan@ysu.edu.cn

[1] State Key Laboratory of Metastable Materials Science and Technology, College of Materials Science and Engineering, Yanshan University, Qinhuangdao 066004, People's Republic of China

are unusual. Furthermore, investigation of the relationship between dielectric relaxation and high energy storage density in biaxially oriented PVDF/PMMA composite films is even rare. Biaxially oriented film is superior in homogeneous of film quality and is the best method for high electric breakdown strength. Our interest focuses on the relationship between dielectric relaxation and high energy storage density in PVDF/PMMA composite films. All dielectric materials do not exhibit all polarizations but varies with different frequency and temperature. Relaxations as a function of temperature and frequency reveal a lot of information on the chemical and physical status of material, which can benefit to the comprehensive understanding of the molecular motions and their relaxation behaviors [20]. Thus, the dielectric relaxation processes of biaxially oriented P(VDF-HFP)/PMMA films are investigated using dielectric relaxation spectroscopy in this paper. The parameters of various relaxations depending on the blending composition are analyzed to reveal the relationship between dielectric relaxation, interactions of PVDF and PMMA and high energy storage density.

2 Experimental section

2.1 Materials

poly(vinylidene fluoride-hexafluoropropylene) [P(VDF-HFP), Kynar Flex 2850-00] pellets was purchased from Arkema corporation, France. Poly(methyl methacrylate) (PMMA, CM-207, $M_n = 38{,}406$ g/mol, $M_w = 72{,}777$ g/mol, $M_w/M_n = 1.9$) pellets were purchased from Chi Mei corporation.

2.2 The fabrication of biaxially oriented P(VDF-HFP)/PMMA composite films

P(VDF-HFP)/PMMA mixtures were compounded using a two-screw extruder with a maximum barrel temperature of 210 °C and pelletized. Subsequently, the composite materials were converted into sheets by hot-pressing at 230 °C, followed by immediate quenching into ice water (0 °C). Biaxially oriented composite films were prepared using the hot-pressed sheets ranging from 0 to 40 % PMMA by weight in a bidirectional synchronous drawing machine (home-made), the composite films were naturally cooled down to room temperature and the thickness is about 20 μm.

2.3 Dielectric and D–E hysteresis loop measurements

Dielectric relaxation spectroscopy (DRS) measurements were performed on a Novocontrol Concept 80 dielectric spectrometer with the frequency ranging from 10 Hz to 10 MHz and the temperature ranging from −100 to 140 °C at 1.0 V. The D–E hysteresis loops were measured on a Premiere II ferroelectric tester from Radiant Technologies. The samples were subjected to a bipolar wave, with frequency of 10 Hz.

3 Results and discussion

Previous studies of the relaxations in PVDF and PMMA show [21–23] that three relaxation processes are observed in crystalline PVDF: (1) the α_a relaxation process, due to segmental motions in the amorphous phase; (2) the α_c relaxation process, associated with the crystalline phase [24]; and (3) the β relaxation process, caused by localized motions.

Dielectric loss (Tanδ) as a function of temperature at different frequency is shown in Fig. 1. Four relaxation peaks are observed: a weak peak, gradually disappear with increasing frequency, is termed β relaxation below glass transition temperature T_g [P(VDF-HFP), ca. −40 °C, the data of Arkema corporation]. Above T_g, a large and broad peak, shifts to a higher temperature with increasing frequency, be defined as α_a relaxation process. Furthermore, the magnitude of α_a relaxation peak increases with increasing frequency and gradually evolve into a single peak at 1.07 MHz. The opposite trend is obtained for a higher temperature peak, which is known as α_c. A new peak is discovered in the low frequency and high temperature, termed conductivity relaxation process.

The imaginary parts (ε″) of complex permittivity as a function of frequency at different temperatures for biaxially oriented P(VDF-HFP) film are shown in Fig. 2. A weak and broad β relaxation process is detected at low

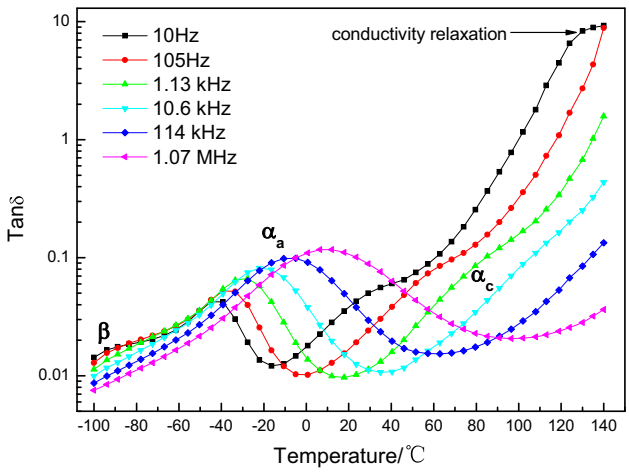

Fig. 1 Dielectric loss (Tanδ) as a function of temperature at different frequencies for biaxially oriented P(VDF-HFP) films

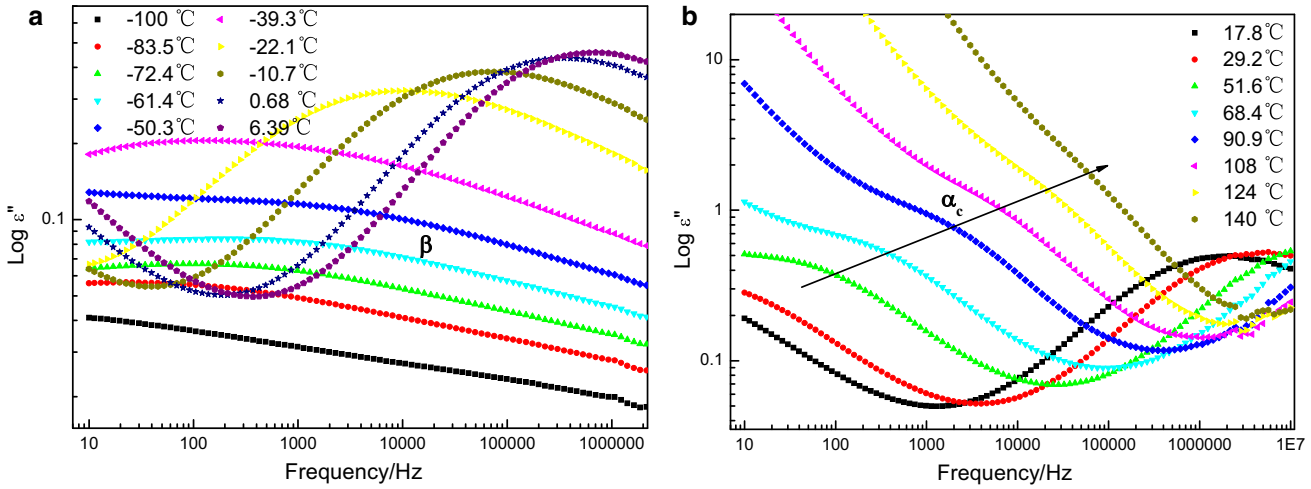

Fig. 2 The imaginary (ε″) part of complex permittivity as a function of frequency at different temperatures (**a** below 15 °C and **b** above 15 °C) for biaxially oriented P(VDF-HFP) films

temperature, as shown in Fig. 2a. Careful inspection of Fig. 1 a reveals that a increase in temperature from −100 to 6.39 °C causes the β relaxation process to evolve into α_a relaxation process. α_a relaxation process is associated with glass transition of P(VDF-HFP) matrix, which shifts to a high frequency with increasing temperature and exceeds the measurement scope above 50 °C (see Fig. 2b). This relaxation process is referred to as a primary relaxation, which, for the dipole moments of view, results from large-range motions of dipole relaxation process corresponding to microbrownian segmental motion of polymer main chain [25]. Dipoles begin to have enough mobility to contribute to an increase in permittivity at the temperature near T_g. Along the arrow of Fig. 2b, α_c relaxation is obvious, which shifts to a high frequency with increasing temperature. Meanwhile the peak intensity of α_c diminishes with increasing temperature. It is associated with various forms of crystal imperfections that include chain loops at the lamellar surface, chain rotations and twisting within the interior of the crystals, discontinuities, etc. [21, 26–28]. At low frequencies and high temperatures, a steep increase is observed, which comes from the dc conductivity. When conductivity dominates the dielectric loss spectra and masks the α_c relaxation peaks at low frequencies (see 140 °C), complex dielectric modulus is often applied to reveal the obscured relaxation process [29–31]. Conductivity relaxation is discussed below.

Tanδ as a function of temperature at different frequency is shown in Fig. 3. PMMA exhibits three relaxation peaks: a weak γ relaxation peak, connected with rotation of the methyl ester side groups [32] appears and shifts to a lower temperature with decreasing frequency between −40 and −100 °C. A strong β relaxation peak, associated with the localized motions of side groups in the glassy state, is

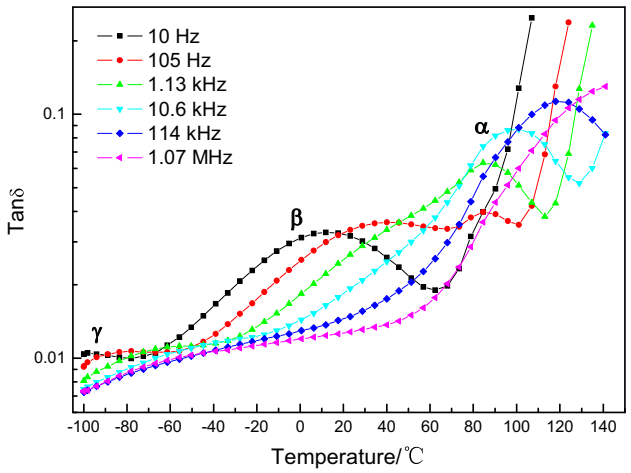

Fig. 3 Dielectric loss (Tanδ) as a function of temperature at different frequencies for pure PMMA films

found below the T_g of PMMA (ca. 105 °C, the data of Chi Mei corp.). The peak of β relaxation shifts to a higher temperature with increasing frequency. The peak of α relaxation occurs at higher temperature and is associated with segmental motions. The peaks of α and β relaxations can be distinguished clearly below 105 Hz. Above 1.13 kHz, α relaxation peak gradually vanishes due to the partial overlap with β relaxation. Eventually the β relaxation merges with the α relaxation to form a single αβ relaxation which is present around and above the T_g. Although conductivity relaxation is not observed in Fig. 3, Tanδ has an abrupt increase at low frequency and high temperature. This results from free charges (impurities) [33].

Figure 4 shows that ε″ as a function of frequency at −39 °C for composite films. −39 °C closes to T_g of

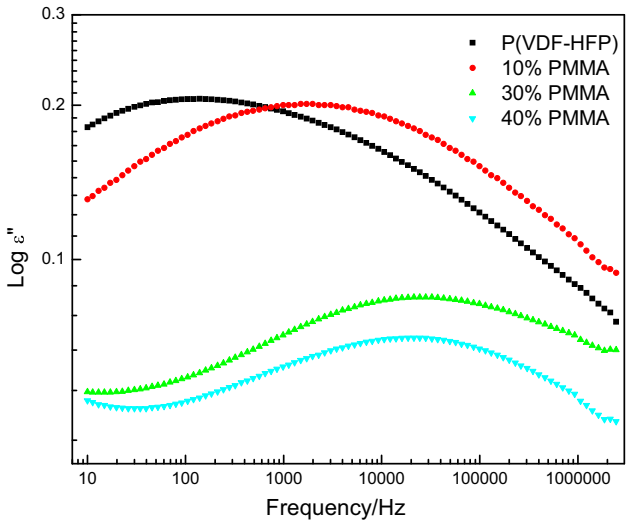

Fig. 4 The imaginary (ε″) part of complex permittivity as a function of frequency at −39 °C for the biaxially oriented composite films with different content of PMMA

P(VDF-HFP), α_a relaxation is primary, and the relaxation of PMMA is almost non-existent or badly weak (see Fig. 3). It is obvious that α_a relaxation peak shifts to a higher frequency, and the relaxation strength of the peak sharply diminishes with increasing PMMA content when compared with pure P(VDF-HFP). The frequencies of α_a peak in Fig. 4 are 139 Hz for pure P(VDF-HFP) film, 1.5 kHz for 10 % PMMA composite film, 21.3 kHz for 30 % PMMA composite film, and 24.5 kHz for 40 % PMMA composite film. Interestingly, α_a peak relaxation time for samples with different PMMA contents comes closer with increasing temperature (Fig. 5). A clearer plot of the relaxation time at maximum ε″ versus reciprocal temperature for biaxially oriented composite films of different PMMA composition is shown in Fig. 6. It is readily observed that the relaxation time of ε″ peak drops sharply with increase of temperature and PMMA content. These indicate that the temperature dependence of α_a relaxation varies with PMMA composition.

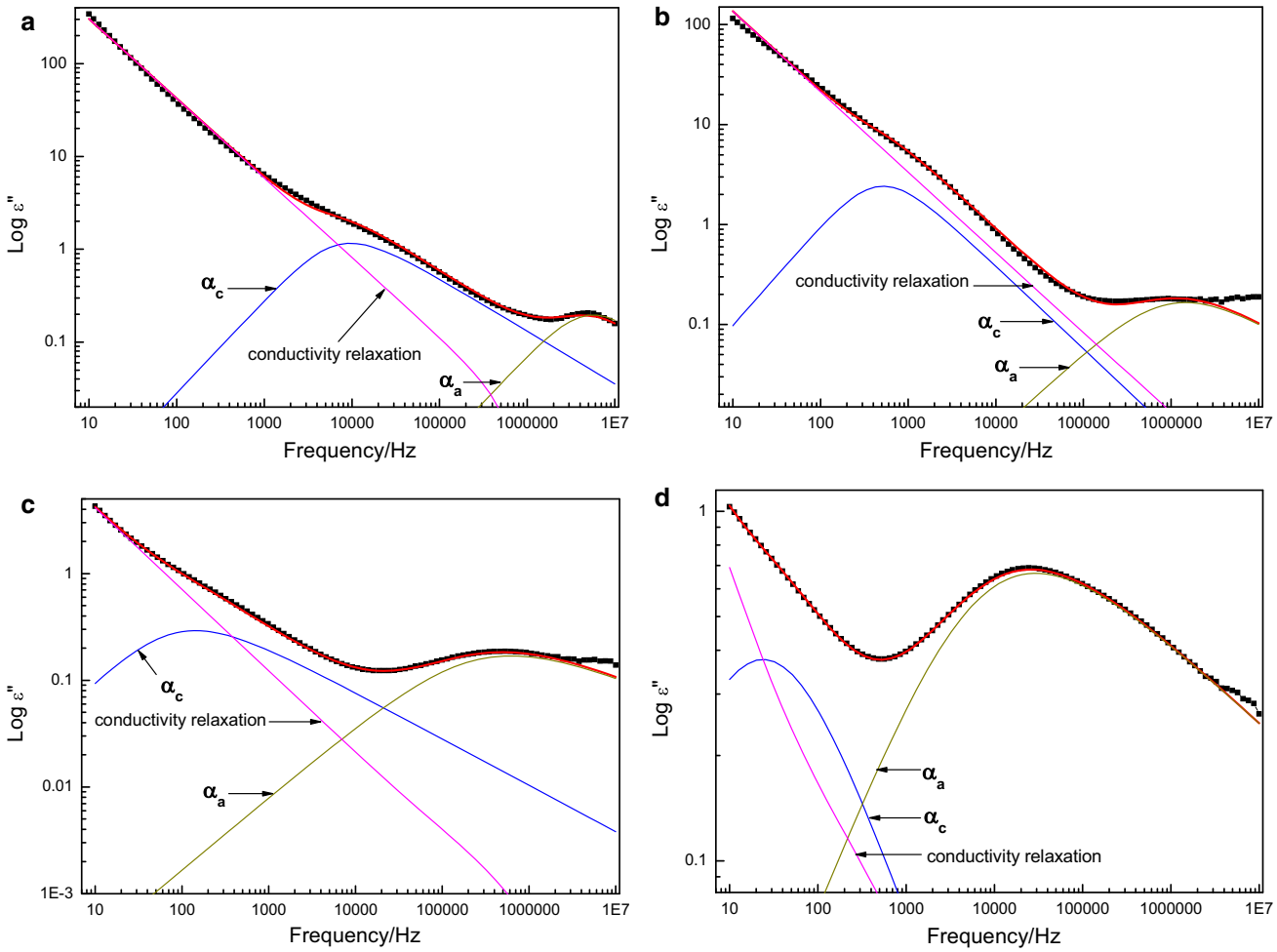

Fig. 5 Decomposition of the ε″ at 123 °C into the α_a, α_c and conductivity relaxation according to HN equation for **a** P(VDF-HFP) film, and **b** 10 % PMMA, **c** 30 % PMMA, **d** 40 % PMMA composite films

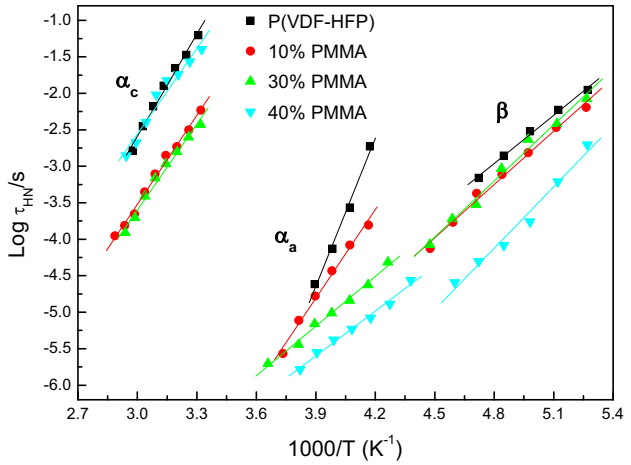

Fig. 6 Relaxation times (Log τ_{HN}) of the β, α_a, α_c processes as a function of reciprocal temperature (1/T) for biaxially oriented composite films of different PMMA composition. The *solid curves* represent Arrhenius fits to β, α_a, α_c relaxation processes, respectively

The α_a, α_c and conductivity relaxation overlapped at higher temperature, their separation is made by using the Havriliak–Negami (HN) function [34]:

$$\varepsilon^* = \varepsilon_\infty + \frac{\Delta\varepsilon}{\left[1 + (i\omega\tau_{HN})^{\alpha_{HN}}\right]^{\gamma_{HN}}} - i\frac{\sigma_0}{\omega^s\varepsilon_0} \quad (1)$$

In the H–N equation, ε* is complex dielectric constant, $\omega = 2\pi f$ is electric field oscillation frequency; ε_∞ is frequency limit of dielectric constant; Δε is dielectric relaxation strength defined as $\Delta\varepsilon = \varepsilon_{s-}\varepsilon_\infty$. τ_{HN} is relaxation time. α_{HN} and γ_{HN} ($0 < \alpha_{HN}$, $\gamma_{HN} \leq 1$) are the shape parameters of the relaxation spectra, $\alpha_{HN} = \gamma_{HN} = 1$ for a Debye relaxation process. The parameter α_{HN} represents the width of the distribution and γ_{HN} describes the asymmetry of this distribution. In the Eq. (1), the added term $-i\frac{\sigma_0}{\omega^s\varepsilon_0}$ stands for conductivity effects, where σ_0 is related to the dc conductivity of the sample and ε_0 is the dielectric constant of vacuum. The exponent *s* represents conduction process.

Figure 5 shows the curve-fitting of an example with regard to the decomposition of the ε″ relaxation peak at 123 °C for P(VDF-HFP) and its composite films. These curves in Fig. 5 are fitted by using Eq. (1). Apparently, the maxima of α_c and α_a relaxations shift to lower frequencies with increasing PMMA content. The width of α_c relaxation peak decreases, but the width of α_a relaxation increases gradually with the rising of PMMA content. These results indicate that the crystallinity of the composite films decreases, amorphous region is dominated. It is consistent with the conclusion of our previous work [35].

The effect of PMMA is further analyzed by the temperature behavior of the relaxation processes mentioned previously for biaxially oriented composite films of different PMMA composition (see Fig. 6). The β, α_a, α_c processes are well described by the Arrhenius equation [36]:

$$\tau_{HN}(T) = \tau_0 \exp(E_a/KT) \quad (2)$$

where τ_{HN} is the mean relaxation time, K is the Boltzmann's constant, τ_0 is the pre-exponential factors, E_a is the activation energy and T is the absolute temperature. According to Fig. 6, the fitted parameters are shown in Table 1. For the β relaxation associated with localized motions, the relaxation time at infinite temperature (Log τ_0) changes from −13.53 s of P(VDF-HFP) to 17.61 s of the composite with 40 % PMMA, while the activation energy (E_a) increases with increasing PMMA content, indicating that the introduction of PMMA has a cooperative effect in a lower temperature (below T_g). Above T_g, the relaxation time and the activation energy (E_a) for α_a relaxation, which associate with segmental motions in the entire amorphous phase, all decrease with the increase of PMMA content These suggest that the addition of PMMA facilitates α_a relaxation, and a lower energy is required for the dipole to follow the change of the frequency. The E_a of α_c process also decrease with increasing PMMA content. The E_a of biaxially oriented composite films for α_c process are significantly lower than the result of the Ref. [15], which reflect more imperfect existing in P(VDF-HFP) crystallites. These results are interpreted by the decrease of crystallinity and crystal size due to the effect of biaxially oriented composite films [35].

Temperature dependencies of the parameters for β, α_a, α_c relaxation, which were obtained after simulation of the overlapping processes according to Eq. (1), are shown in Figs. 7 and 8. The character of the fitted data essentially changes in the transition region from the local mobility in the glass state to the segmental mobility above T_g. Thus, it

Table 1 Parameters of Arrhenius equation for biaxially oriented P(VDF-HFP)/PMMA composite films

Relaxation	Sample	Log τ_0 (s)	E_a (kJ/mol)
β	P(VDF-HFP)	−13.53 ± 0.42	18.31 ± 0.08
	10 % PMMA	−14.94 ± 0.50	20.25 ± 0.10
	30 % PMMA	−15.50 ± 0.61	21.29 ± 0.12
	40 % PMMA	−17.61 ± 0.98	23.35 ± 0.19
α_a	P(VDF-HFP)	−31.05 ± 1.92	56.28 ± 0.48
	10 % PMMA	−20.63 ± 0.78	33.72 ± 0.19
	30 % PMMA	−14.03 ± 0.36	18.85 ± 0.09
	40 % PMMA	−13.58 ± 0.39	17.01 ± 0.09
α_c	P(VDF-HFP)	−16.60 ± 0.68	38.84 ± 0.22
	10 % PMMA	−15.72 ± 0.39	33.83 ± 0.13
	30 % PMMA	−15.37 ± 0.61	32.60 ± 0.19
	40 % PMMA	−14.26 ± 0.99	32.42 ± 0.32

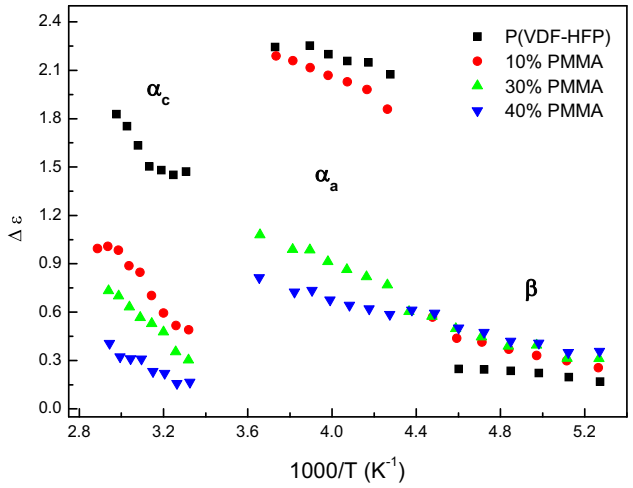

Fig. 7 Dielectric relaxation strength (Δε) versus reciprocal temperature for different relaxations of biaxially oriented composite films of different PMMA composition

is seen that dielectric relaxation strength (Δε) noticeably increases above T_g (about −40 °C). Below T_g, the Δε of P(VDF-HFP) is lower than the composite films due to the cooperation effect of side groups for PMMA and P(VDF-HFP). But, the Δε of the composite films rapidly decreases when compared with pure P(VDF-HFP) at the temperature above T_g due to the dilution effect of PMMA, the decrease of crystallinity and crystal size of P(VDF-HFP). This behavior can be further discussed with the Kirkwood–Fröhlich equation [37], which has been used to describe the relationship between dielectric relaxation strength and the parameters involved in the dielectric relaxation processes through:

$$\Delta\varepsilon = \frac{1}{3\varepsilon_0} g \frac{\mu^2}{k_B T} \frac{N}{V} = \frac{1}{3\varepsilon_0} g \frac{\mu^2}{k_B T} \frac{\rho_A N_A}{M} \tag{3}$$

where Δε is the dielectric relaxation strength; ε_0 is the vacuum dielectric constant; g represents the intermolecular

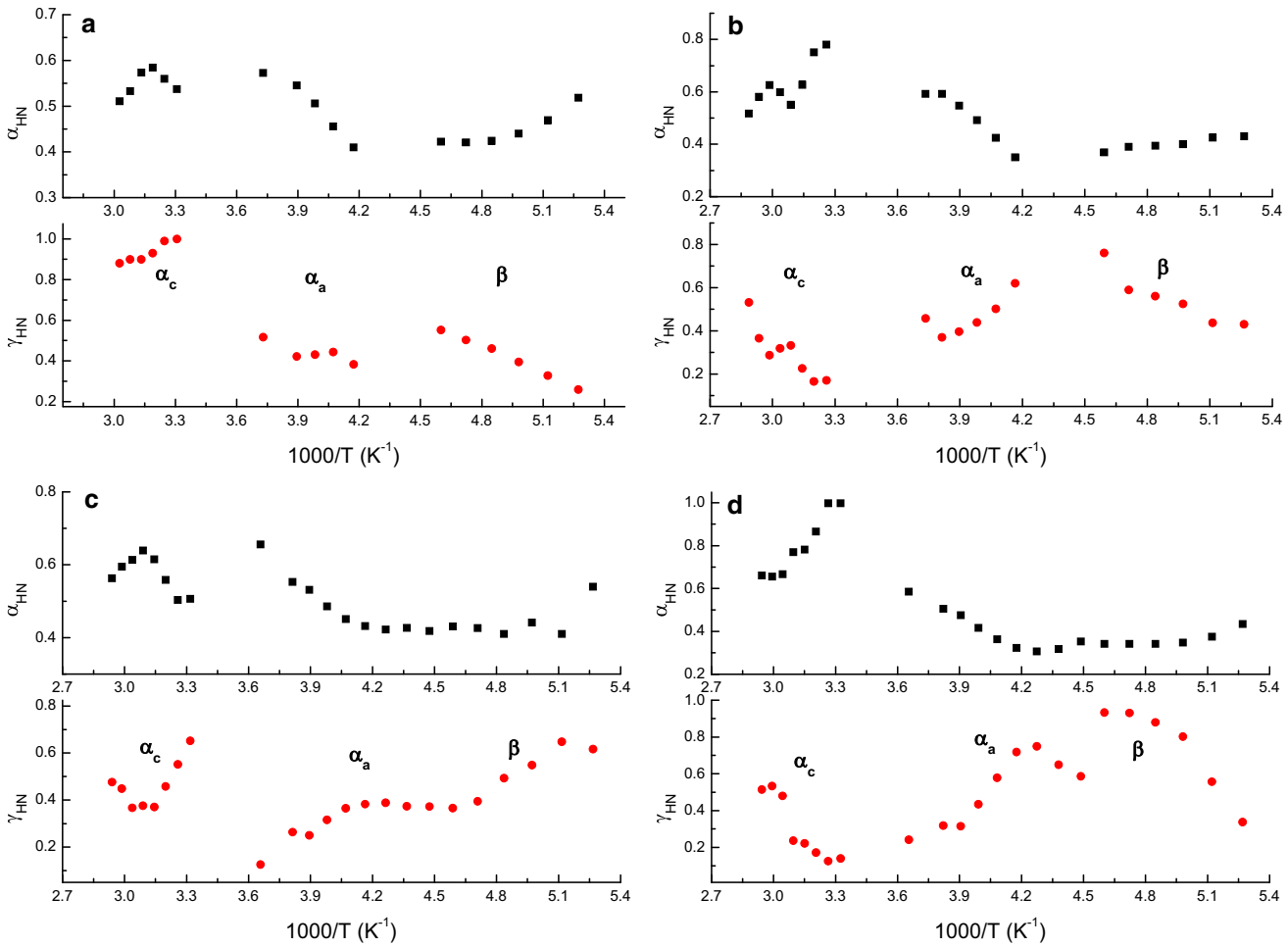

Fig. 8 The fitted shape parameters, α_{HN} and γ_{HN}, versus reciprocal temperature of different relaxations for biaxially oriented **a** P(VDF-HFP) film, and **b** 10 % PMMA, **c** 30 % PMMA, **d** 40 % PMMA composite films

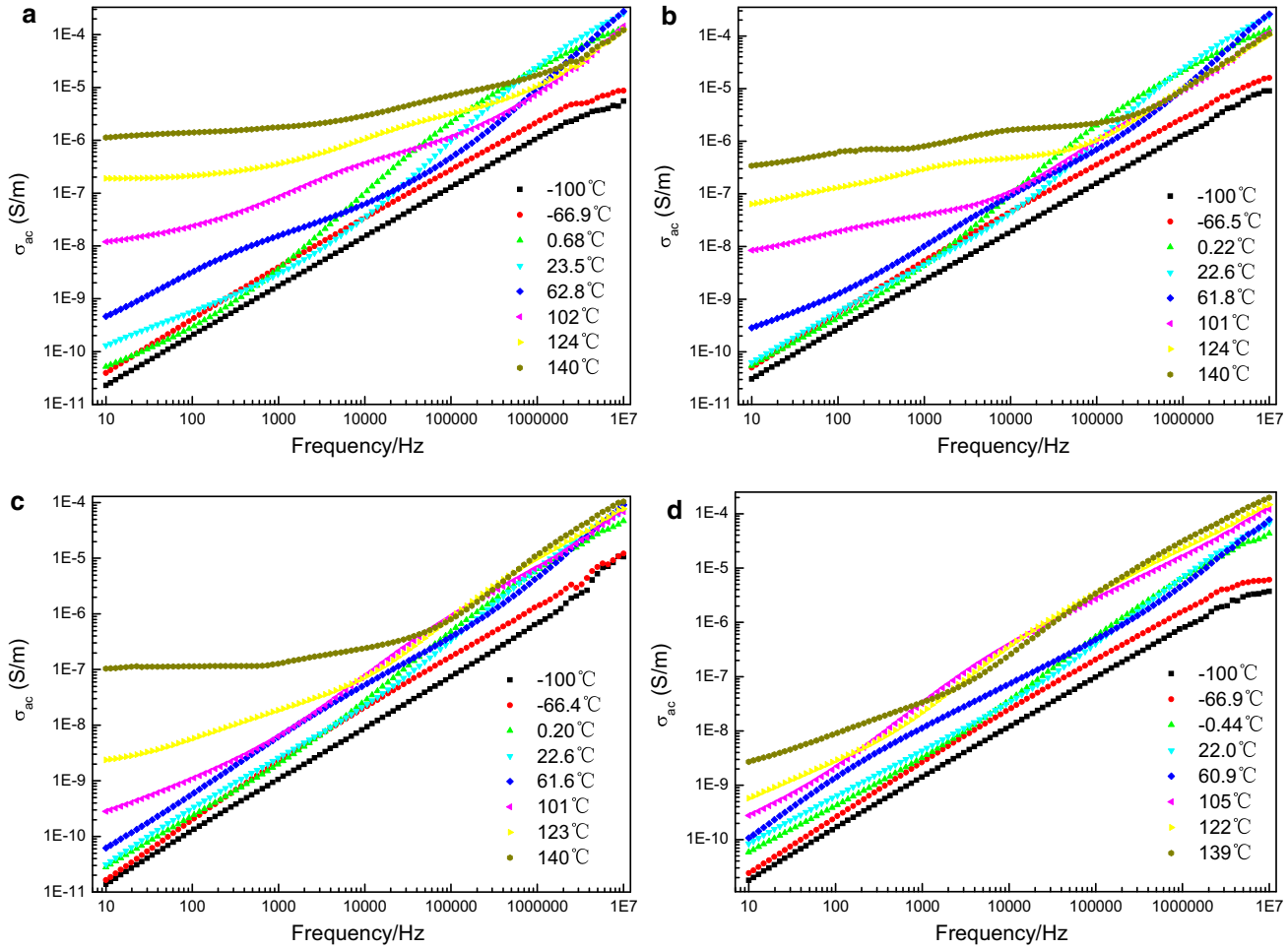

Fig. 9 AC conductivity versus frequency for biaxially oriented **a** P(VDF-HFP) film, and **b** 10 % PMMA, **c** 30 % PMMA, **d** 40 % PMMA composite films at different temperatures

interaction between dipoles involved in the dielectric relaxation; μ is the mean dipole moment related to the process under consideration; k_B is Boltzmann's constant; N/V is the number density of dipoles contributing to the concerned dielectric relaxation; ρ_A is the mass density; M is the molecular weight of the material involved in the relaxation process; and N_A is Avogadro's constant.

We use α_a relaxation as an example to interpret our viewpoints. α_a relaxation, associated with the amorphous phase, refers to dipoles in the amorphous regions. Thus, ρ_A is the mass density of the amorphous P(VDF-HFP). Considering other factors to be constant in Eq. (3), and Eq. (3) can be simplified to: $\Delta\varepsilon \approx g\mu^2/T$. Furthermore, we assume that the mean dipole moments of the amorphous phases of P(VDF-HFP) and PMMA do not vary in biaxially oriented P(VDF-HFP)/PMMA composite films systems, so Δε is proportional to the product of g and amount of dipole moments. Figure 7 shows that the temperature dependence of α_a dielectric relaxation strength (Δε). Obviously, Δε decrease with the amount of PMMA increases. The DSC and XRD results of our previous work showed that the degree of crystallinity of the composite films decreased when compared with neat P(VDF-HFP), which means that the amount of dipole moments in amorphous regions increases. Thus, we conclude that the correlation factor g must decrease with the introduction of PMMA. The decrease of g suggests a weaker intermolecular interaction and antiparallel alignment due to dipole cancellation effects in the composite films [38]. But on the contrary, the increase of parallel alignment leads to an enhancement of the effective dipole moment. This result induces the decrease of the mean relaxation time (τ_{HN}) and dielectric relaxation strength (Δε) for α_a process. In Fig. 7 also shows that enhancement of Δε with temperature. As the dipole moment do not varies with temperature, the correlation factor g increases with temperature, indicating that the interaction between dipoles in the amorphous regions is raised or the parallel alignment for dipoles enhanced with increasing temperature. In addition, Fig. 8 shows the shape

parameters, α_{HN} and γ_{HN}, versus temperature for different relaxations. Apparently, all the values of α_{HN} and γ_{HN} of the three relaxations are between 0 and 1, which means the relaxation processes of the biaxially oriented P(VDF-HFP) and its composite films belong to non-debye model relaxation. Namely, each relaxation includes multiple relaxation processes of microstructure.

Next, we shall discuss the conductivity (σ), which is mentioned earlier in this article. Conductivity (σ) in P(VDF-HFP) and its composite films under high electric fields and high temperatures should be closely related to the orientation of amorphous/crystalline dipoles, ionic polarization, and injected charges [39]. Conductivity (σ) of polymer is classified into two different processes [40, 41]. DC conductivity (σ_{dc}) is a result of the localized charges jumping to neighboring sites, which form a continuous connected network, allowing the charges to travel through the entire physical dimensions of the sample; AC conductivity (σ_{ac}) does not demand a percolation path through the sample and is a result of reciprocating movement like a jumping dipole. σ_{ac} is often found to obey the form [42]: $\sigma_{ac} = \sigma_{dc} + A\omega^s$. We do not discuss this formula here. The σ_{ac} in Figs. 9 and 10 is obtained by following formula: $\sigma_{ac} = \omega\varepsilon_0\varepsilon''$, where ε_0 is the permittivity of free space (8.854×10^{-12} F/m), ω is the angular frequency ($\omega = 2\pi f$). In Fig. 9, the σ_{dc} of P(VDF-HFP) and its composite films increase with increasing frequency and temperature. We observe that the σ_{dc} of all films can not be observed below room temperature, which because the mobility of impurity ions is fairly slow around and below room temperature [43]. Figure 10 shows AC conductivity versus frequency for biaxially oriented neat P(VDF-HFP) and P(VDF-HFP)/PMMA composite films at 140 °C. At the low frequency range, the σ_{ac} of the composite films sharply decreases with the addition of PMMA. Compared with neat P(VDF-HFP), the σ_{ac} of 40 % PMMA film reduces by about three orders of magnitude. In addition, for samples with more PMMA, the σ_{ac} increases more rapidly with the increases of frequency, which can be considered effects of the dominating dipole polarization of the amorphous regions. This because amorphous regions increase with PMMA increased, and crystalline regions are not melted entirely at 140 °C.

Typical Dielectric materials will show a D–E hysteresis loop to illustrate its ferroelectric behavior, as shown in Fig. 11 for the biaxially oriented P(VDF-HFP) and its composite films. Obviously, the area of D–E hysteresis loop rapidly decreases with the addition of PMMA. It also can be seen that the values of remanent polarization (P_r) and coercive field markedly reduces from 3.8 μC/cm^2 and 125.8 MV/m for P(VDF-HFP) film to 1.3 μC/cm^2 and 23.4 MV/m for 40 % PMMA film, respectively. These measures are around the room temperature, and the results have been closely related with α_a relaxation. The decreases of dielectric relaxation strength ($\Delta\varepsilon$) and correlation factor g can benefits the drop of P_r with increasing PMMA content. In addition, the lower the activation energy (E_a) facilitates the switching of effective dipoles for amorphous segments, which makes coercive field decrease. Further, the lower conductivity could not form a percolation path under high electric field, and the breakdown strength could be enhanced continuously (see Table 2). The energy storage property of the biaxially oriented composite film need to be further researched below T_g or above room temperature. According to the analysis above, we could design the microstructure of dielectric materials to obtain the films with high energy storage density.

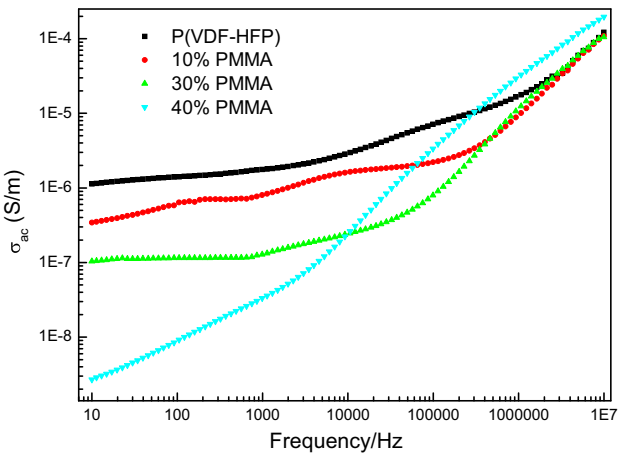

Fig. 10 AC conductivity versus frequency for biaxially oriented neat P(VDF-HFP) and P(VDF-HFP)/PMMA composite films at 140 °C

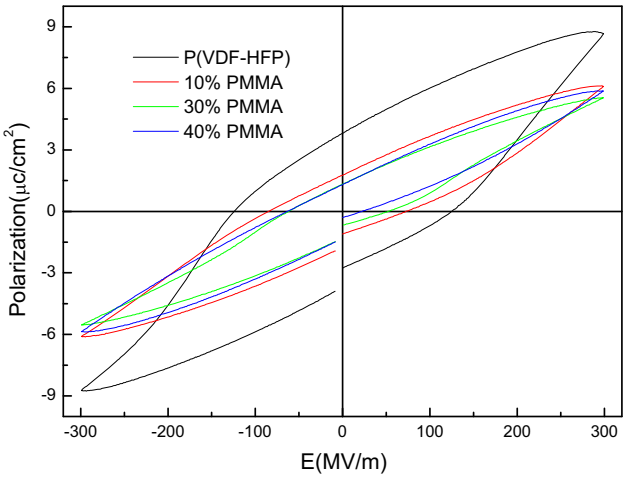

Fig. 11 Bipolar D–E hysteresis loops of biaxially oriented P(VDF-HFP)/PMMA composite films at room temperature and frequency of 10 Hz

Table 2 The breakdown strengths of biaxially oriented P(VDF-HFP)/PMMA composite films

Materials	Shape parameter (k)	Breakdown strength (E_0, MV/m)
P(VDF-HFP)	10.38	449.97
10 % PMMA	19.92	530.53
30 % PMMA	17.10	539.26
40 % PMMA	18.29	549.38

The breakdown strength was analyzed by a two-parameter Weibull distribution function: $P(E) = 1 - \exp[-(E/E_0)^k]$, where P(E) is the cumulative probability of failure occurring at the electric field equal to E. E_0 is the field strength for which there is a 63 % probability for the sample to breakdown, while the shape parameter (k) evaluates the scatter of data ($\geq$10)

4 Conclusions

Semicrystalline P(VDF-HFP)/PMMA composite films were prepared via biaxially oriented technique. We have investigated the dielectric relaxation processes in P(VDF-HFP), PMMA, and a series of P(VDF-HFP)/PMMA composite films in detail by dielectric relaxation spectroscopy. The β relaxation of P(VDF-HFP) which was caused by localized motions appears below T_g, while the activation energy (E_a) and dielectric relaxation strength ($\Delta\varepsilon$) slightly increased with the addition of PMMA. The α_a relaxation which was induced by segmental motions in the amorphous phase of P(VDF-HFP) and PMMA began around and above T_g. The α_c relaxation, associated with the crystalline phase, occurred mainly above room temperature. Both E_a and $\Delta\varepsilon$ of α_a and α_c relaxations significantly decreased with increasing PMMA content. The three relaxations all belonged to non-debye model. Moreover, the conductivities (σ) of P(VDF-HFP)/PMMA composite films decreased sharply with the increase of PMMA content. The decrease of dielectric relaxation strength ($\Delta\varepsilon$) benefits the drop of P_r, lower the activation energy (E_a) makes coercive field decrease and the lower conductivity (σ) could enhances the breakdown strength. Thus, the area of D–E hysteresis loop rapidly decreases with the addition of PMMA.

Acknowledgments This work was funded by Natural Science Foundations of Hebei Province of China (E2012203153).

References

1. R. Gregorio Jr., M. Cestari, Effect of crystallization temperature on the crystalline phase content and morphology of poly(vinylidene fluoride). J. Polym. Sci. Part B Polym. Phys. **32**, 859–870 (1994)
2. K.P. Pramoda, A. Mohamed, I.Y. Phang, T. Liu, Crystal transformation and thermomechanical properties of poly(vinylidene fluoride)/clay nanocomposites. Polym. Int. **54**, 226–232 (2005)
3. T. Mizutani, T. Yamada, M. Ieda, Thermally stimulated currents in polyvinylidene fluoride. I. Unstretched alpha-form PVDF. J. Phys. D Appl. Phys. **14**, 1139–1147 (1981)
4. T. Furukawa, A.J. Lovinger, G.T. Davis, M.G. Broadhurst, Dielectric hysteresis and nonlinearity in a 52/48 molcopolymer of vinylidene fluoride and trifluoroethylene. Macromolecules **16**, 1885–1890 (1983)
5. T. Furukawa, Ferroelectric properties of vinylidene fluoride copolymers. Phase Transit. **18**, 143–211 (1989)
6. X. Zhou, B. Chu, B. Neese, M. Lin, Q.M. Zhang, Electrical energy density and discharge characteristics of a poly(vinylidene fluoride-chlorotrifluoroethylene)copolymer. IEEE Trans. Dielectr. Electr. Insul. **14**, 1133–1138 (2007)
7. X. Zhou, X. Zhao, Z. Suo, C. Zou, J. Runt, S. Liu, S. Zhang, Q.M. Zhang, Electrical breakdown and ultrahigh electrical energy density in poly(vinylidene fluoride-hexafluoro-propylene) copolymer. Appl. Phys. Lett. **94**, 162901–162903 (2009)
8. J.J. Li, S.B. Tan, S.J. Ding, H.Y. Li, L.J. Yang, Z.C. Zhang, High-field antiferroelectric behaviour and minimized energy loss in poly(vinylidene-co-trifluoroethylene)-graft-poly (ethyl methacrylate) for energy storage application. J. Mater. Chem. **22**, 23468–23476 (2012)
9. Q.J. Meng, W.J. Li, Y.S. Zheng, Z.C. Zhang, Effect of poly(-methyl methacrylate) addition on the dielectric and energy storage properties of poly(vinylidene fluoride). J. Appl. Polym. Sci. **116**, 2674–2684 (2010)
10. N. Chen, L. Hong, Surface phase morphology and composition of the casting films of PVDF–PVP blend. Polymer **43**, 1429–1436 (2002)
11. H.H. Yang, C.D. Han, J.K. Kim, Rheology of miscible blends of poly(methyl methacrylate) with poly(styrene-co-acrylonitrile) and with poly(vinylidene fluoride). Polymer **35**, 1503–1511 (1994)
12. T. Nishi, T.T. Wang, Melting point depression and kinetic effects of cooling on crystallization in poly(vinylidene fluoride)–poly(-methyl methacrylate) mixtures. Macromolecules **8**, 909–915 (1975)
13. T.T. Wang, T. Nishi, Spherulitic crystallization in compatible blends of poly(vinylidene fluoride) and poly(methyl methacrylate). Macromolecules **10**, 421–425 (1977)
14. H. Zhang, K. Lamnawar, A. Maazouz, Rheological modeling of the mutual diffusion and the interphase development for an asymmetrical bilayer based on PMMA and PVDF model compatible polymers. Macromolecules **46**, 276–299 (2013)
15. Y.X. Zhang, M. Zuo, Y.H. Song, X.P. Yan, Q. Zheng, Dynamic rheology and dielectric relaxation of poly(vinylidene fluoride)/poly(methyl methacrylate) blends. Compos. Sci. Technol. **106**, 39–46 (2015)
16. X.J. Zhao, J. Cheng, J. Zhang, S.J. Chen, X.L. Wang, Crystallization behavior of PVDF/PMMA blends prepared by in situ polymerization from DMF and ethanol. J. Mater. Sci. **47**, 3720–3728 (2012)
17. B. Charlot, S. Gauthier, A. Garraud, P. Combette, A. Giani, PVDF/PMMA blend pyroelectric thin films. J. Mater. Sci. Mater. Electron. **22**, 1766–1771 (2011)
18. G.R. Peng, X.J. Zhao, Z.J. Zhan, S.Z. Ci, Q. Wang, Y.J. Liang, M.L. Zhao, New crystal structure and discharge efficiency of poly(vinylidene fluoride-hexafluoropropylene)/poly(methyl methacrylate) blend films. RSC Adv. **4**, 16849–16854 (2014)
19. M.Y. Li, N. Stingelin, J.J. Michels, M.J. Spijkman, K. Asadi, K. Feldman, P.W.M. Blom, D.M. de Leeuw, Ferroelectric phase

diagram of PVDF: PMMA. Macromolecules **45**, 7477–7485 (2012)
20. P. Saxena, M.S. Gaur, P.K. Khare, R.K. Tiwari, Dielectric relaxation in polyvinylidene-fluoride–polysulfone blends. J. Electrostat. **69**, 214–219 (2011)
21. J. Mijovic, J.W. Sy, T.K. Kwei, Reorientational dynamics of dipoles in poly(vinylidene fluoride)/poly(methyl methacrylate) (PVDF/PMMA) blends by dielectric spectroscopy. Macromolecules **30**, 3042–3050 (1997)
22. J.W. Sy, J. Mijovic, Reorientational dynamics of poly(vinylidene fluoride)/poly(methyl methacrylate) blends by broad-band dielectric relaxation spectroscopy. Macromolecules **33**, 933–946 (2000)
23. S. Maya, S. Keshav, B. Suryasarathi, Segmental relaxations and crystallization-induced phase separation in PVDF/PMMA blends in the presence of surface-functionalized multiwall carbon nanotubes. J. Phys. Chem. B **117**, 8589–8602 (2013)
24. H. Rekik, Z. Ghallabi, I. Royaud, M. Arous, G. Seytre, G. Boiteux, A. Kallel, Dielectric relaxation behaviour in semi-crystalline polyvinylidene fluoride (PVDF)/TiO_2 nanocomposites. Compos. Part B Eng. **45**, 1199–1206 (2013)
25. Y. Ishida, M. Watanabe, K. Yamafuji, Dielectric behavior of polyvinylidene fluoride. Kolloid Z **200**, 48 (1964)
26. K. Nakagawa, Y. Ishida, Annealing effects in poly(vinylidene fluoride) as revealed by specific volume measurements, differential scanning calorimetry, and electron microscopy. J. Polym. Sci. Part B Polym. Phys. **11**, 2153–2171 (1973)
27. K. Naoki, A. William, I.I.I. Goddard, Dielectric properties of poly(vinylidene fluoride) from molecular dynamics simulations. Macromolecules **16**, 6765–6772 (1995)
28. M. Arous, I.B. Amor, A. Kallel, Z. Fakhfakh, G. Perrier, Crystallinity and dielectric relaxations in semi-crystalline poly(ether ether ketone). J. Phys. Chem. Solids **68**, 1405–1414 (2007)
29. H.K. Lee, S. Pejanovic, I. Mondragon, J. Mijovic, Dynamics of single-walled carbon nanotube (SWNT)/polyisoprene (PI) nanocomposites in electric and mechanical fields. Polymer **48**, 7345–7355 (2007)
30. F.Q. Tian, Y. Ohki, Electric modulus powerful tool for analyzing dielectric behavior. IEEE Trans. Dielectr. Electr. Insul. **21**, 929–931 (2014)
31. X.J. Zhao, G.R. Peng, X.B. Jiang, W.P. Liu, Z.J. Zhan, W.N. Meng, Y.C. Wang, T.X. Song, J. Li, H.Y. Feng, Investigation of relaxation process in poly(vinylidene fluoride-hexafluoropropylene) using dielectric relaxation spectroscopy. J. Mater. Sci. Mater. Electron. **27**, 718–723 (2016)
32. Y. Lin, Y. Shangguan, M. Zuo, E. Harkin-Jones, Q. Zheng, Effects of molecular entanglement on molecular dynamics and phase-separation kinetics of poly(methyl methacrylate)/poly(-styrene-co-maleic anhydride) blends. Polymer **53**, 1418–1427 (2012)
33. H. Hammami, M. Arous, M. Lagache, A. Kallel, Experimental study of relaxations in unidirectional piezoelectric composites. Compos. Part A Appl. S. **37**, 1–8 (2006)
34. V.V. Kochervinskij, I.A. Malyshkina, N.P. Bessonova, S.N. Suljanov, K.A. Dembo, Effect of recrystallization on the molecular mobility of a copolymer of vinylidene fluoride and hexafluoropropylene. J. Appl. Polym. Sci. **120**, 13–20 (2011)
35. X.J. Zhao, G.R. Peng, Z.J. Zhan, W.N. Meng, X.B. Jiang, J. Li, T.X. Song, Y.C. Wang, W.P. Liu, Structure change and energy storage property of poly(vinylidene fluoride-hexafluoropropylene)/poly (methyl methacrylate) blends. Polym. Sci. Ser. A **57**, 452–459 (2015)
36. M.D. Migahed, F. Fahmy, Structural relaxation around the glass transition temperature in amorphous polymer blends: temperature and composition dependence. Polymer **35**, 1688–1693 (1994)
37. L. Yu, P. Cebe, Effect of nanoclay on relaxation of poly(vinylidene fluoride) nanocomposites. J. Polym. Sci. Part B Polym. Phys. **47**, 2520–2532 (2009)
38. X. Li, Z.M. Chen, Z.J. Li, Y.Q. Gao, W.K. Tu, X.Q. Li, Y.Q. Zhang, Y.D. Liu, L.M. Wang, Comparative study of dynamics in glass forming mixtures of Debye-type Nethylacetamide with water, alcohol, and amine. J. Chem. Phys. **141**, 1045061–1045068 (2014)
39. L.Y. Yang, J. Ho, E. Allahyarov, R.R. Mu, L. Zhu, Semicrystalline structure-dielectric property relationship and electrical conduction in a biaxially oriented poly(vinylidene fluoride) film under high electric fields and high temperatures. ACS Appl. Mater. Interfaces **7**, 19894–19905 (2015)
40. G.M. Tsangaris, G.C. Psarras, N. Kouloumbi, Electric modulus and interfacial polarization in composite polymeric systems. J. Mater. Sci. **33**, 2027–2037 (1998)
41. S.R. Eliotta, AC Conduction in amorphous chalcogenide and pnictide semiconductors. Adv. Phys. **36**, 135–218 (1987)
42. A.S. Nowich, B.S. Lim, A.V. Vaysleyb, Nature of the ac conductivity of ionically conducting crystals and glasses. J. Non Cryst. Solids **172–174**, 1243–1251 (1994)
43. J.K. Tseng, S. Tang, Z. Zhou, M. Mackey, J.M. Carr, R. Mu, L. Flandin, D.E. Schuele, E. Baer, L. Zhu, Interfacial polarization and layer thickness effect on electrical insulation in multilayered polysulfone/poly(vinylidene fluoride) films. Polymer **55**, 8–14 (2014)